Article

Cell Reports

NLRX1 Acts as an Epithelial-Intrinsic Tumor Suppressor through the Modulation of TNF-Mediated Proliferation

Graphical Abstract

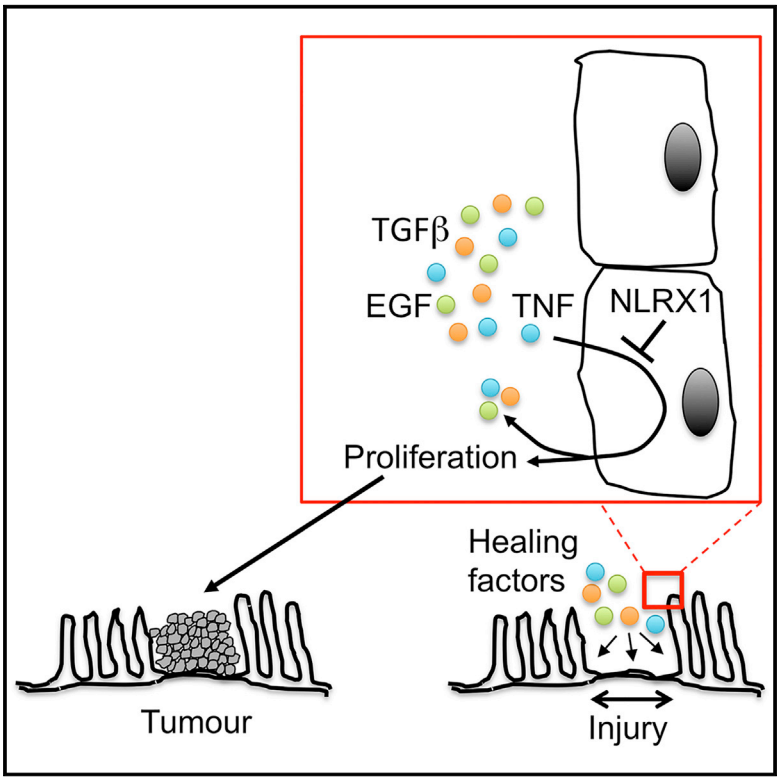

Authors

Ivan Tattoli, Samuel A. Killackey, Elisabeth G. Foerster, ..., Catherine J. Streutker, Dana J. Philpott, Stephen E. Girardin

Correspondence

stephen.girardin@utoronto.ca

In Brief

NLRX1 protects against colorectal tumorigenesis. Tattoli et al. now examine the mechanism underlying this effect and find that epithelial NLRX1 protects against colitis-associated colorectal cancer. In the epithelium, NLRX1 controls the expression of intestinal wound healing factors following injury and inhibits the proliferative action of TNF.

Highlights

- Epithelial NLRX1 protects against colorectal cancer
- NLRX1 dampens expression of intestinal wound healing factors
- NLRX1 inhibits proliferation during epithelial regeneration post-colitis
- In organoids, NLRX1 inhibits TNF-induced proliferation and signaling

Tattoli et al., 2016, Cell Reports *14*, 2576–2586
March 22, 2016
http://dx.doi.org/10.1016/j.celrep.2016.02.065

OPEN ACCESS
CellPress

Cell Reports
Article

NLRX1 Acts as an Epithelial-Intrinsic Tumor Suppressor through the Modulation of TNF-Mediated Proliferation

Ivan Tattoli,[1,2] Samuel A. Killackey,[1] Elisabeth G. Foerster,[2] Raphael Molinaro,[1] Charles Maisonneuve,[2] Muhammed A. Rahman,[1,2] Shawn Winer,[4] Daniel A. Winer,[4] Catherine J. Streutker,[1,3] Dana J. Philpott,[2] and Stephen E. Girardin[1,*]

[1]Department of Laboratory Medicine and Pathobiology
[2]Department of Immunology
[3]Saint Michael's Hospital
[4]Department of Pathology, Toronto General Hospital
University of Toronto, M5S 1A8 Toronto, Canada
*Correspondence: stephen.girardin@utoronto.ca
http://dx.doi.org/10.1016/j.celrep.2016.02.065

SUMMARY

The mitochondrial Nod-like receptor protein NLRX1 protects against colorectal tumorigenesis through mechanisms that remain unclear. Using mice with an intestinal epithelial cells (IEC)-specific deletion of *Nlrx1*, we find that NLRX1 provides an IEC-intrinsic protection against colitis-associated carcinogenesis in the colon. These Nlrx1 mutant mice have increased expression of *Tnf*, *Egf*, and *Tgfb1*, three factors essential for wound healing, as well as increased epithelial proliferation during the epithelial regeneration phase following injury triggered by dextran sodium sulfate. In primary intestinal organoids lacking *Nlrx1*, stimulation with TNF resulted in exacerbated proliferation and expression of the intestinal stem cell markers *Olfm4* and *Myb*. This hyper-proliferation response was associated with increased activation of Akt and NF-κB pathways in response to TNF stimulation. Together, these results identify NLRX1 as a suppressor of colonic tumorigenesis that acts by controlling epithelial proliferation in the intestine during the regeneration phase following mucosal injury.

INTRODUCTION

NLRX1 is a member of the Nod-like receptor (NLR) family of intracellular sensors of danger-associated molecular patterns (DAMPs) and microbial-associated molecular patterns (MAMPs) that function in innate immunity (Philpott et al., 2014). In contrast to other members of the NLR family, NLRX1 possesses an N-terminal addressing sequence that targets the protein to the mitochondrial matrix (Arnoult et al., 2009). The exact function of NLRX1 has remained poorly understood. It was proposed to act as a negative regulator of antiviral immunity through interaction with the protein MAVS (Moore et al., 2008), but these findings were not reproduced by other groups (Jaworska et al., 2014; Rebsamen et al., 2011; Soares et al., 2013). Overexpression of NLRX1 was also shown to regulate the formation of reactive oxygen species (ROS) by mitochondria (Tattoli et al., 2008). Further support for this observation was obtained in mouse embryonic fibroblasts (MEFs) from *Nlrx1*$^{-/-}$ mice, which displayed blunted tonic levels of ROS in resting condition as compared to wild-type (WT) MEFs (Soares et al., 2014).

NLRX1 was also shown to inhibit inflammatory pathways triggered by lipopolysaccharide (Allen et al., 2011; Xia et al., 2011). Moreover, *Nlrx1*$^{-/-}$ mice display increased cerebral inflammation in a model of experimental autoimmune encephalopathy (Eitas et al., 2014), higher lung inflammation in a model of cigarette smoke-induced chronic obstructive pulmonary disease (Kang et al., 2015), and enhanced intestinal inflammation in a colitis model induced by dextran sodium sulfate (DSS) (Soares et al., 2014). However, the underlying mechanism through which NLRX1 controls inflammation in these various models remains unclear.

Recently, findings from several groups have identified a role for NLRX1 in the control of cell death in various cellular systems (Imbeault et al., 2014; Jaworska et al., 2014; Singh et al., 2015; Soares et al., 2014). However, it remains unclear if the effect of NLRX1 on ROS or cell death signaling is direct or whether it is a consequence of an overarching function of the protein in the mitochondria that remains to be identified. In support of the latter hypothesis, it must be noted that NLRX1 expression is significantly repressed by glucose starvation (Soares et al., 2014); in addition, NLRX1 silencing is sufficient to upregulate the basal activities of complex I and III of the mitochondrial respiratory chain (Singh et al., 2015), suggesting that NLRX1 may act to tie mitochondrial oxidative

phosphorylation (Oxphos) activity to the cellular availability of glucose. As such, NLRX1 could play a role as a tumor suppressor by inhibiting mitochondrial Oxphos-dependent generation of ATP in conditions of nutrient sufficiency. This hypothesis is supported by several lines of evidence. First, *NLRX1* expression is strongly reduced by SV40- or Ras-dependent transformation in a genome-wide study (Danielsson et al., 2013), a result that we confirmed by analyzing *Nlrx1* expression by qPCRand western blotting in primary versus in SV40-transformed MEFs (Soares et al., 2014). Second, we recently demonstrated that *Nlrx1*$^{-/-}$ mice display increased susceptibility to tumorigenesis in a model of colitis-associated colorectal cancer triggered by injection of azoxymethane (AOM) followed by three cycles of oral administration of DSS in drinking water (Soares et al., 2014). Finally, Singh et al. (2015) demonstrated that *NLRX1* expression decreases tumorigenic and migration properties of MCF-7 cells in vitro and the tumorigenic potential of colon cancer RKO cells in vivo using a xenograft model in nude mice.

While the critical role of NLRX1 in tumorigenesis is increasingly appreciated, the underlying mechanism remains unclear. In the AOM/DSS model of colorectal cancer, it is well established that inflammation is a major driver of tumor progression, as DSS administration strongly accelerates pathogenesis as compared to injection of AOM alone (Rosenberg et al., 2009). Because DSS-induced inflammation is increased in animals lacking *Nlrx1* (Soares et al., 2014), the enhanced tumor burden observed in *Nlrx1*$^{-/-}$ in the AOM/DSS model as compared to WT mice could be caused by uncontrolled inflammation. Alternatively, NLRX1's proposed role in the control of apoptosis and mitochondrial respiration, as well as its transcriptional regulation by glucose levels and during cellular transformation, argue for a cell intrinsic effect of NLRX1 on tumorigenesis. In order to delineate the exact mechanism through which NLRX1 protects against colorectal cancer, we generated mice lacking *Nlrx1* only within the intestinal epithelium. Our results demonstrated an epithelial-intrinsic role of NLRX1 in the control of colitis-associated tumorigenesis. We present evidence that NLRX1 played its protective role by inhibiting TNF-induced intestinal epithelial cell (IEC) proliferation, which occurs during the healing phase post-colitis.

RESULTS

Generation and Analysis of Mice Lacking *Nlrx1* in the Intestinal Epithelium

C57Bl/6 mice with insertion of LoxP sites flanking Exon 3 of *Nlrx1* (*Nlrx1*$^{fl/fl}$ hereafter) have been described previously (Soares et al., 2013). We crossed these mice with transgenic C57Bl/6 mice expressing the Cre recombinase under the *Villin* gene promoter in order to excise *Nlrx1* specifically in IECs (Figure S1A). *Nlrx1*$^{-/-}$, WT, *Nlrx1*$^{fl/fl}$ mice as well as mice with homozygous deletion of *Nlrx1* in IECs (*Nlrx1*$^{\Delta IEC}$ thereafter) were analyzed for NLRX1 expression in the spleen and the intestinal mucosa by western blotting (Figure 1A). As expected, only *Nlrx1*$^{-/-}$ mice lost immunoreactivity for NLRX1 in the spleen. In intestinal mucosal samples of *Nlrx1*$^{\Delta IEC}$ mice, NLRX1 expression was absent from the IEC fraction, but not the remaining lamina propria fraction, indicating that *Nlrx1* deletion was specific to the IEC population. We also noted that NLRX1 expression in the spleen and the lamina propria was similar between WT and *Nlrx1*$^{fl/fl}$ mice (Figure 1A), thus showing that LoxP sites insertion in the *Nlrx1* locus had no overall effect on *Nlrx1* expression.

Next, we aimed to determine if *Nlrx1*$^{\Delta IEC}$ mice had intestinal defects in resting conditions. Importantly, for these experiments and the ones described in the rest of this study, *Nlrx1*$^{fl/fl}$ and *Nlrx1*$^{\Delta IEC}$ mice were littermates from *Nlrx1*$^{fl/fl}$×*Nlrx1*$^{\Delta IEC}$ mice crosses. Histology of the colon (Figure 1B) revealed normal crypt architecture in *Nlrx1*$^{\Delta IEC}$ mice and no signs of inflammation. IEC proliferation, as assessed by Ki-67 staining (Figures 1C and 1D) and analysis of Cyclin D1 and Cyclin B1 expression by quantitative (q)PCR, was also unaffected by *Nlrx1* deletion (Figure 1D). Immunofluorescence using an antibody against chromogranin A revealed a normal number of enteroendocrine cells in the colonic epithelium of *Nlrx1*$^{\Delta IEC}$ mice (Figures 1E and S1C) and expression of *Chga*, *Gcg*, and *Cck*, three markers of enteroendocrine cells, was also normal in the colon of *Nlrx1*$^{\Delta IEC}$ mice (Figure 1F). Alcian Blue-Periodic acid-Schiff (AB-PAS) staining and immunofluorescence staining using an antibody against Muc2 also showed that goblet cell numbers were unaffected in *Nlrx1*$^{\Delta IEC}$ mice (Figures 1G, S1B, and S1C), although analysis of *Muc2* expression by qPCR revealed increased expression in *Nlrx1*$^{\Delta IEC}$ mice (Figure 1H). Together, these results show that deletion of *Nlrx1* in IECs does not significantly alter intestinal architecture.

Expression of *Nlrx1* in the Intestinal Epithelium Protects against Colitis-Associated Tumorigenesis

We previously reported that whole-body deletion of *Nlrx1* exacerbated colitis-associated tumorigenesis in the AOM/DSS model (Soares et al., 2014), but whether this effect was epithelium-intrinsic or due to increased inflammation was not addressed. *Nlrx1*$^{fl/fl}$ and *Nlrx1*$^{\Delta IEC}$ mice received an intraperitoneal injection of AOM (10 mg/kg) followed by three cycles of DSS (2.5% in drinking water). In both male and female cohorts of mice receiving AOM/DSS treatment, animals lost weight during DSS cycles, which they recovered during the intercycles (Figure 2A). A trend toward increased weight loss in *Nlrx1*$^{fl/fl}$ mice as compared to *Nlrx1*$^{\Delta IEC}$ mice was observed. Colon shortening, an indication of intestinal inflammation, was observed in both *Nlrx1*$^{fl/fl}$ and *Nlrx1*$^{\Delta IEC}$ mice, although it appeared to be slightly more pronounced in *Nlrx1*$^{fl/fl}$ mice (Figure 2B). Moreover, histological analysis of colon sections showed no significant difference overall between *Nlrx1*$^{fl/fl}$ and *Nlrx1*$^{\Delta IEC}$ mice with regards to inflammation-associated parameters (Figure 2C). In particular, sub-mucosal edema, tissue damage, polymorphonuclear (PMN) infiltration and hyperplasia were similar between both groups of mice. However, analysis of tumor burden showed that AOM-DSS treated *Nlrx1*$^{\Delta IEC}$ mice developed approximately twice as many tumors as *Nlrx1*$^{fl/fl}$ mice (Figure 2D) and histopathological scoring of these tumors revealed an increased number of adenomas in *Nlrx1*$^{\Delta IEC}$ mice (Figures 2E and 2F).

The above results suggest that the impact of *Nlrx1* deficiency on tumorigenesis is epithelial-intrinsic and not driven by changes

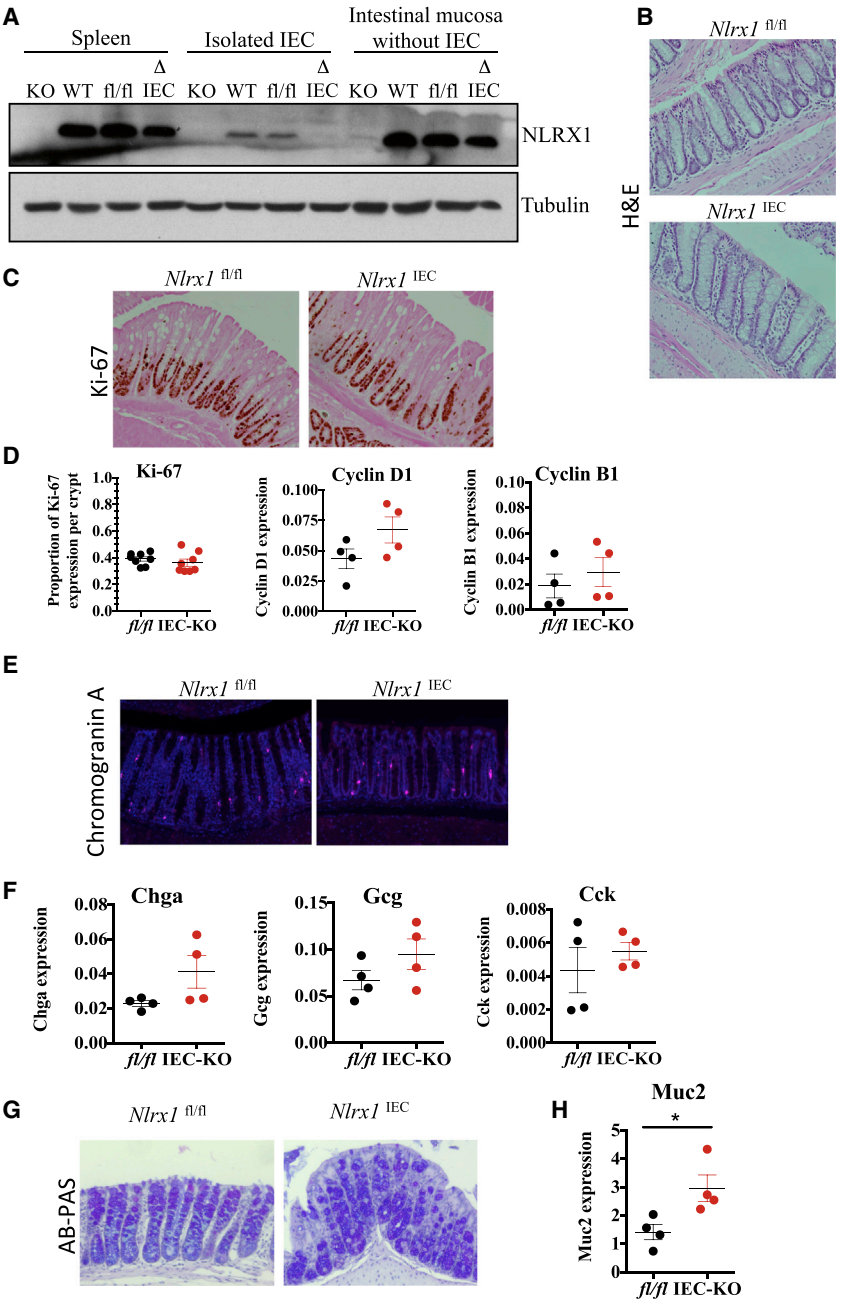

Figure 1. Generation and Analysis of Mice Lacking *Nlrx1* in the Intestinal Epithelium

(A) Western blot analysis of NLRX1 and Tubulin (loading control) in spleen, isolated IEC fraction, and intestinal mucosa depleted of IECs from *Nlrx1*$^{-/-}$ (KO), WT mice, *Nlrx1*$^{fl/fl}$ (fl/fl), and *Nlrx1* $^{\Delta IEC}$ (ΔIEC) mice.

(B–H) Colonic tissue was collected from *Nlrx1*$^{fl/fl}$ and *Nlrx1* $^{\Delta IEC}$ (IEC-KO) mice and processed for H&E staining (B), IHC using anti-Ki-67 antibody (C), qPCR for Ki-67, *Cyclin D1*, and *Cyclin B1* (D), *Chga*, *Gcg*, and *Cck* (F), or *Muc2* (H), immunofluorescence using anti-chromogranin A (Chga) antibody (E), or AB-PAS staining (G). For qPCR data, each point represents the average value for one mouse obtained as a technical triplicate. The images presented in (B), (C), and (E) are representative of data analyzed on n ≥ 4 mice. *p < 0.05 and other comparisons showed no statistical difference.

in the inflammatory environment. In agreement with a cancer cell-intrinsic role of NLRX1, publically available data show that expression of *NLRX1* is lower in tumors than the normal corresponding tissue in human cancers, including bladder, cervical, esophageal, colon, and skin cancers (Figure S2A). Moreover, analysis of two large data sets of colorectal cancer demonstrated that *NLRX1* expression was significantly reduced in colon adenocarcinoma or colon mucinous adenocarcinoma as compared to normal colon (Figure S2B). Finally, analysis of 1,010 human cancer cell lines (from the Cancer Cell Line Encyclopedia) showed that the cell line with the lowest expression of *NLRX1* was NCI-H716, which is derived from a colon adenocarcinoma (Figure S2C). Thus, available data from human cancer and cancer cell lines indicate that *NLRX1* expression is reduced in multiple cancers and in particular in colon cancer.

Mutations in the Adenomatous polyposis coli (*APC*) gene are found in sporadic colon cancers in humans (Raskov et al., 2014) and result in uncontrolled Wnt signaling and proliferation of IECs. Mice harboring the *Apc*^{min} mutation develop spontaneous tumors in the small intestine and in the colon (Su et al., 1992). *Nlrx1*-deficient mice were crossed with mice carrying the *Apc*^{min} mutation. Interestingly, *Apc*$^{min/+}$ *Nlrx1*$^{-/-}$ mice had a significantly reduced lifespan and had to be euthanized at age 101.1 ± 8.38 days as compared to littermate *Apc*$^{min/+}$ *Nlrx1*$^{+/+}$ mice that survived until day 132.5 ± 6.39 (Figures 3A and 3B). Moreover, *Apc*$^{min/+}$ *Nlrx1*$^{-/-}$ mice had more colonic tumors and those were larger than the ones observed in *Apc*$^{min/+}$ *Nlrx1*$^{+/+}$ mice (Figures 3C and 3D). Thus, NLRX1 protects against tumorigenesis induced by dysregulation of the Apc/Wnt signaling axis.

Together, these results suggest that NLRX1 acts in an epithelial-intrinsic manner to suppress colorectal tumorigenesis.

Epithelial-Specific Deletion of *Nlrx1* Does Not Affect Peak Tissue Damage Induced by DSS, but Potentiates Expression of Late Tissue Healing Factors TNFα and TGFβ

In order to better understand how IEC-specific deletion of *Nlrx1* contributes to tumorigenesis susceptibility in the colitis-associated AOM/DSS model, DSS-induced colitis was analyzed in *Nlrx1*$^{fl/fl}$ and *Nlrx1*$^{\Delta IEC}$ mice. Following treatment with 2.5%

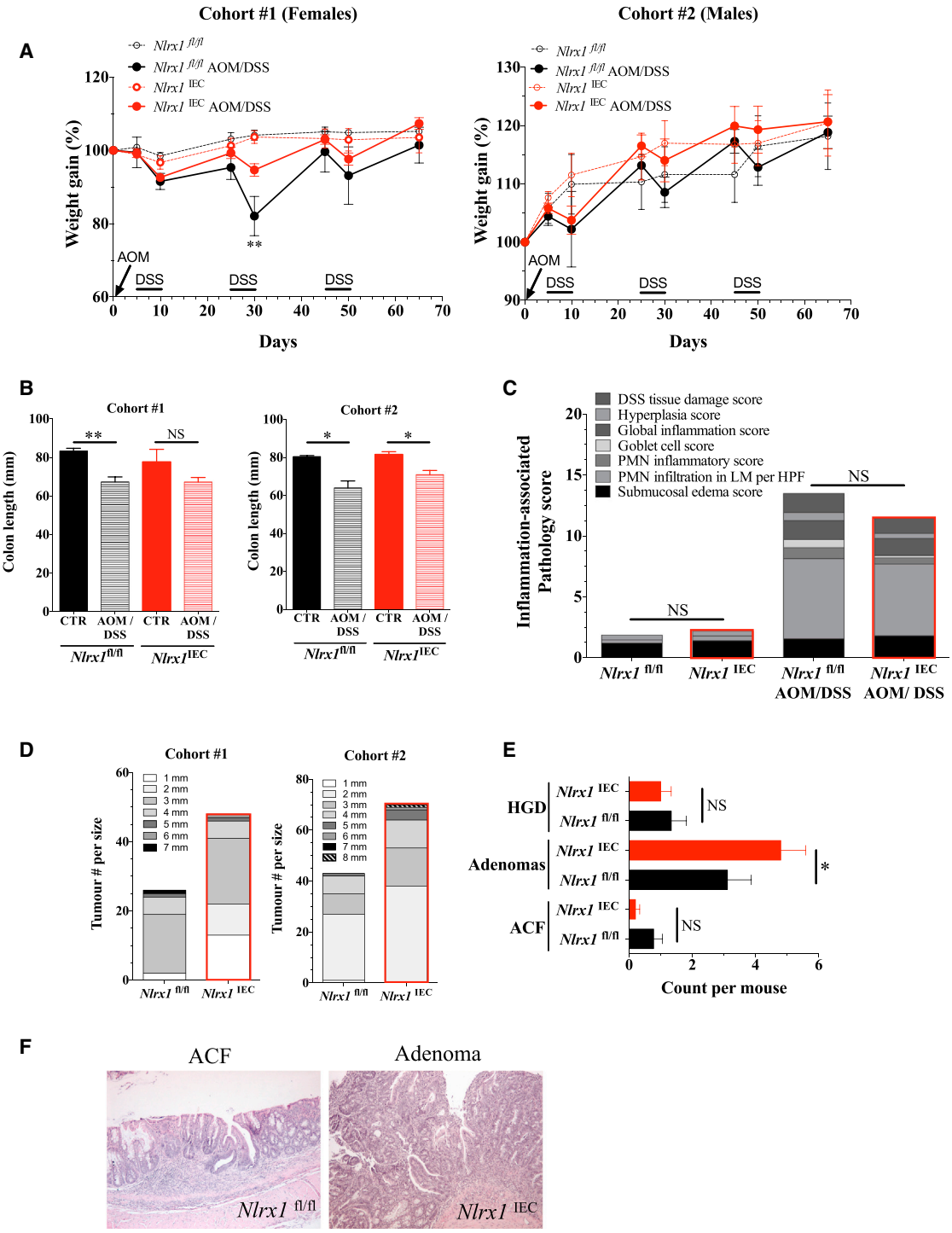

Figure 2. Expression of *Nlrx1* in the Intestinal Epithelium Protects against Colitis-Associated Tumorigenesis

Two independent studies were performed in *Nlrx1*$^{fl/fl}$ and *Nlrx1* $^{\Delta IEC}$ mice to analyze the effect of AOM/DSS on tumorigenesis. Cohorts #1 and #2 were littermate females and males, respectively, either left untreated ($n \geq 3$) or receiving AOM/DSS treatment ($n \geq 7$).

(A) Weight curves.

(B) Measurement of colon length.

(C) Histopathological evaluation of inflammation-associated parameters.

(D and E) Breakdown of the tumor number per size (diameter) (D) and by grade (E).

(F) Representative micrographs showing polyps in colons from AOM/DSS-treated mice (aberrant crypt foci, ACF and high grade dysplasia, HGD) (non-significant, NS) (*$p < 0.05$ and **$p < 0.01$).

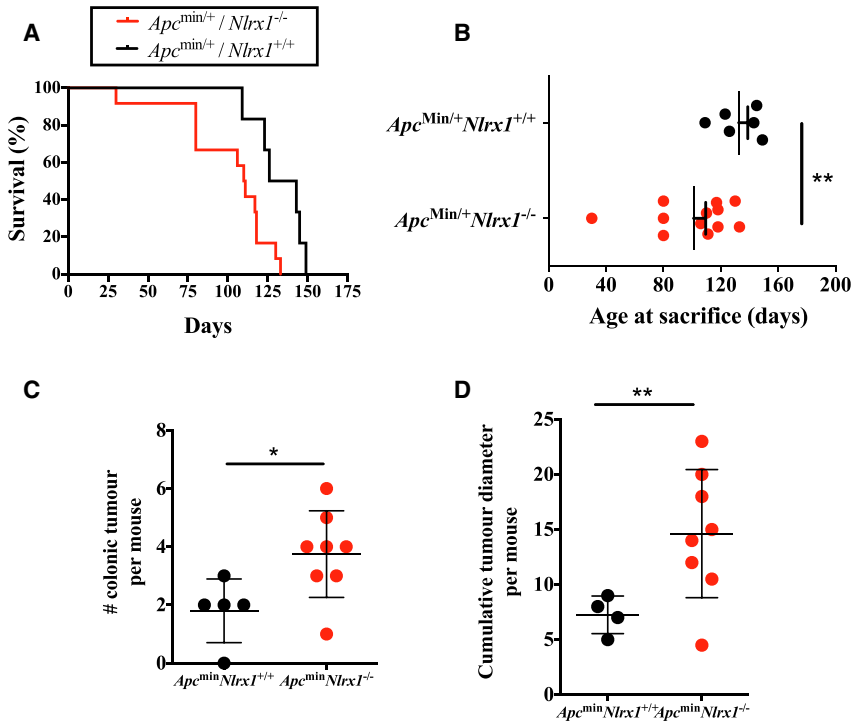

Figure 3. *Nlrx1* Protects against Tumorigenesis in Apc$^{min/+}$ Mice

Analysis of *Apc*$^{min/+}$ *Nlrx1*$^{+/+}$ (n = 6) versus *Apc*$^{min/+}$ *Nlrx1*$^{-/-}$ mice (n = 12).

(A) Survival curve.

(B) Age in days at sacrifice. Tumors were analyzed for animals sacrificed between days 100–150.

(C) Total number of colonic tumors per mouse.

(D) Cumulative tumor size per mouse (*p < 0.05 and **p < 0.01).

DSS in drinking water for 5 days, both groups of mice lost weight similarly, up to day 7 (i.e., 2 days after removal of DSS from drinking water) (Figure 4A). From that time point, both animal groups recovered weight progressively, indicative of a healing process, but *Nlrx1*$^{\Delta IEC}$ mice recovered faster during the d10–d15 period (Figure 4A). Despite this difference in the recovery from DSS-induced colitis, inflammation appeared to be comparable between the two groups of mice, as evidenced by similar colon length at sacrifice (Figure 4B), histology (Figure 4C), blinded inflammatory scores on colonic sections (Figure 4D), levels of keratinocyte chemoattractant or CXCL1 in the serum (Figure S3A), and of secreted IL-1b from intestinal explants in culture (Figure S3B). Of note, this analysis further showed that the peak of intestinal erosion and inflammation was observed at day 7 in both *Nlrx1*$^{fl/fl}$ and *Nlrx1*$^{\Delta IEC}$ mice, which correlates well with the weight loss data (see Figure 4A), but suggests that the faster recovery of *Nlrx1*$^{\Delta IEC}$ mice is independent from inflammation. Next, we performed qPCR analysis on colon mucosa samples from DSS-treated *Nlrx1*$^{fl/fl}$ and *Nlrx1*$^{\Delta IEC}$ mice at day 7 and d12. At the peak of tissue damage (day 7), inflammation-associated genes such as *A20*, *Il10*, and *Il6* were transcriptionally upregulated in both groups of mice and this activation persisted, at least partially up to d12 (Figures S3C–S3E). Although we noted a trend for increased upregulation of *Il6* at day 7 and d12 in *Nlrx1*$^{\Delta IEC}$ mice as compared to *Nlrx1*$^{fl/fl}$ mice, this effect was not significant. Moreover, *Il22* and *Il22ra1* were transiently upregulated at day 7, but this induction was similar between *Nlrx1*$^{fl/fl}$ and *Nlrx1*$^{\Delta IEC}$ mice (Figures S3F and S3G). Interestingly, while *Tnf*, *Egf*, and *Tgfb1* were not transcriptionally upregulated at day 7 in either group of mice, we observed a delayed upregulation of these genes at d12, and this upregulation was significantly more robust in *Nlrx1*$^{\Delta IEC}$ mice as compared to *Nlrx1*$^{fl/fl}$ mice (Figures 4E–4G). Previous work demonstrated that microbial products, in synergy with Notch signaling, could potentiate *Tnf* expression in the intestine (Hu et al., 2008). Interestingly, Notch signaling was activated early (day 7) during colitis as evidenced by the upregulation of the Notch target *Hey1*, and this induction was significantly more pronounced in *Nlrx1*$^{\Delta IEC}$ mice than *Nlrx1*$^{fl/fl}$ mice (Figure S3H). At d12, Notch signaling was still active since expression of *Atoh1*, which is inhibited by Notch, was more blunted in *Nlrx1*$^{\Delta IEC}$ mice than *Nlrx1*$^{fl/fl}$ mice (Figure S3I). Thus, early upregulation of Notch signaling could account, at least in part, for the increased upregulation of *Tnf* observed in *Nlrx1*$^{\Delta IEC}$ mice during colitis.

TNF, EGF, and TGFβ have well-characterized roles in promoting the healing of the intestinal epithelium following injury (Leppkes et al., 2014; Sturm and Dignass, 2008). In particular, TNF stimulates the proliferation of IEC, TGFβ potentiates their migration, and EGF promotes both. Thus, these results suggest that *Nlrx1* deficiency in IEC does not impact the initial wave of induction of inflammatory mediators, which likely originate from immune cells of the lamina propria, but upregulates second-wave mediators involved in tissue healing such as TNF, EGF, and TGFβ.

Increased Epithelial Proliferation in *Nlrx1*$^{\Delta IEC}$ Mice during Epithelial Regeneration

Treatment with DSS results in a massive epithelial erosion and healing requires upregulation of IEC proliferation and migration. Because we observed increased expression of TNF in *Nlrx1*$^{\Delta IEC}$ mice during the regeneration phase following DSS treatment (see above), we aimed to analyze epithelial proliferation.

Immunohistochemistry (IHC) staining using anti-Ki-67, a marker of cellular proliferation, revealed that an increased number of epithelial cells were proliferative in the crypts of *Nlrx1*$^{\Delta IEC}$ mice as compared to *Nlrx1*$^{fl/fl}$ mice at d12 and d20 post-DSS treatment (Figures 5A–5C). It must be noted that at the peak of DSS-induced tissue damage (day 7), the epithelium was too eroded to perform analysis of Ki-67. In the AOM/DSS-treated animals analyzed above (see Figure 2), which were sacrificed at d20 of the third DSS cycle, a similar increase in the number of

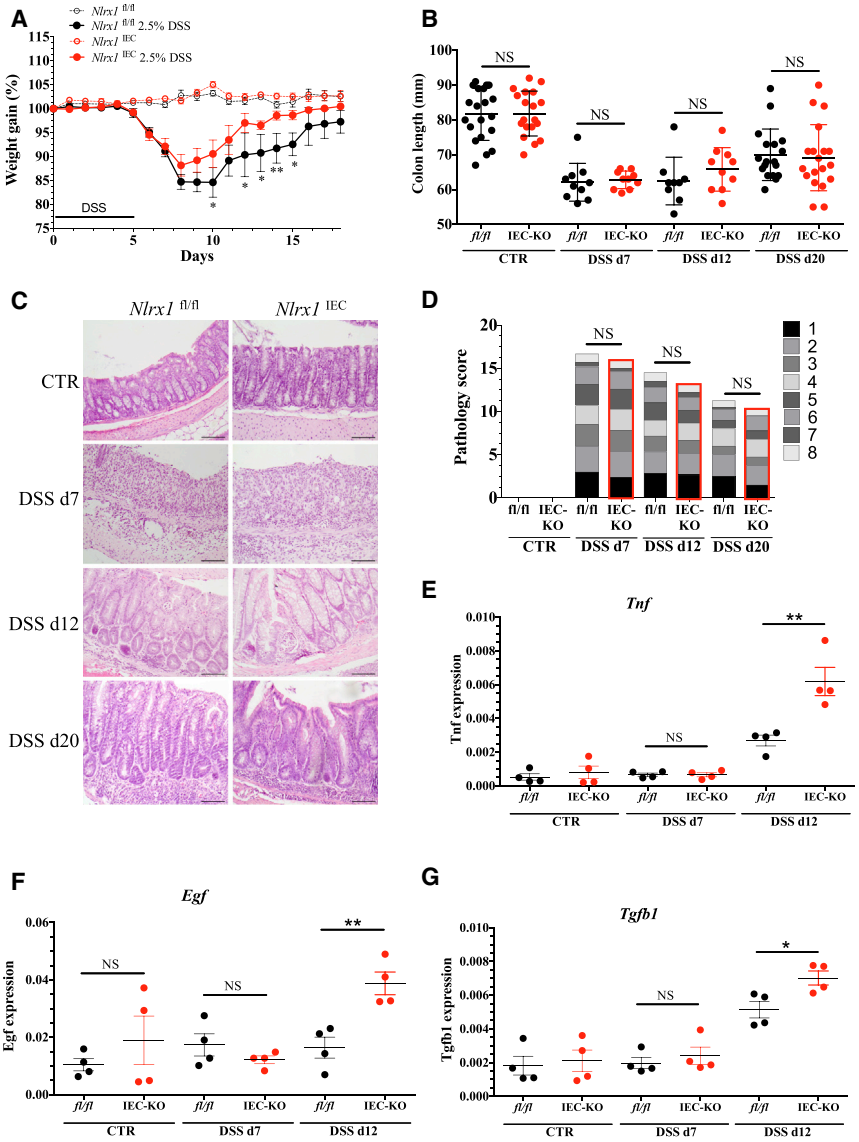

Figure 4. Epithelial-Specific Deletion of *Nlrx1* Does Not Affect Peak Tissue Damage Induced by DSS, but Potentiates Expression of Late Tissue Healing Factors TNFα and TGFβ

Nlrx1$^{fl/fl}$ and *Nlrx1* $^{\Delta IEC}$ mice were challenged with 2.5% DSS for 5 days in drinking water.

(A) Weight curves.

(B) Measurement of colon length of animals sacrificed at day 7 (5 days DSS/2 days recovery in normal water), d12 (5 days DSS/7 days recovery), and d20 (5 days DSS/15 days recovery).

(C) Representative H&E micrographs of colons of animals unchallenged (CTR) or challenged with DSS at day 7, d12, and d20.

(D) Histopathological evaluation of inflammation-associated parameters. The numbers on the right side of the image: 1, total area affected; 2, destruction of mucosal architecture; 3, % severe destruction; 4, degree of cellular infiltration; 5, % severely affected; 6, muscle thickening; 7, crypt abscess; and 8, goblet cell depletion.

(E–G) qPCR analysis of *Tnf* (E), *Egf* (F), and *Tgfb1* (G) in colonic tissues of animals unchallenged (CTR) or challenged with DSS at day 7, d12, and d20. Each point represents the average value for one mouse obtained as a technical triplicate. (*$p < 0.05$ and **$p < 0.01$). (non-significant, NS).

Expression of NLRX1 Inhibits TNF-Mediated Proliferation and Signaling in Primary Intestinal Organoids

In order to gain insights into the mechanism through which epithelial-intrinsic expression of NLRX1 inhibits epithelial proliferation during the regeneration phase post-DSS, we isolated intestinal crypts and cultured primary intestinal organoids from *Nlrx1*$^{fl/fl}$ and *Nlrx1*$^{\Delta IEC}$ mice in Matrigel, as previously described (Sato et al., 2009). Since we observed increased expression of TNF in the colons of *Nlrx1*$^{\Delta IEC}$ mice as compared to *Nlrx1*$^{fl/fl}$ mice during the epithelial regeneration phase (see Figure 4), we hypothesized that TNF could contribute to the hyper-proliferative response observed in *Nlrx1*$^{\Delta IEC}$ mice recovering from DSS. TNF stimulation for 24 hr of freshly passaged organoids from *Nlrx1*$^{fl/fl}$ mice resulted in a modest non-significant increase in the diameter of the organoids (Figures 6A and 6B). In contrast, TNF stimulation more than doubled the surface of organoids from *Nlrx1*$^{\Delta IEC}$ mice (Figures 6A and 6B), and those also had more numerous and longer digitations, showing that these structures displayed increased crypt growth. Next, TNF-stimulated organoids were pulsed with EdU, which incorporates into proliferative cells, and analyzed by flow cytometry. Interestingly, organoids from *Nlrx1*$^{\Delta IEC}$ mice displayed more EdU^{+} cells than those from *Nlrx1*$^{fl/fl}$ mice (Figures 6C and 6D), thus showing that the increase in organoid size following

Ki-67^{+} cells was observed in the crypts of *Nlrx1*$^{\Delta IEC}$ mice as compared to *Nlrx1*$^{fl/fl}$ mice (Figure 5D).

In resting conditions, epithelial cell death must approximately be equal to proliferation in order to keep colonic crypt length constant. Because we previously showed that NLRX1 controls apoptotic cell death, we sought to determine if the more robust proliferation observed in DSS-treated *Nlrx1*$^{\Delta IEC}$ IECs was the result of increased apoptosis. IHC analysis of apoptosis using an antibody against the cleaved form of caspase-3 showed an increase in apoptosis in the colonic crypts of d12 DSS-treated mice as compared to unchallenged animals, but this increase was similar between *Nlrx1*$^{fl/fl}$ and *Nlrx1*$^{\Delta IEC}$ mice (Figures 5E and 5F), thus ruling out the possibility that increased proliferation in DSS-treated *Nlrx1*$^{\Delta IEC}$ mice was a compensation mechanism for enhanced apoptotic cell death. Together, these results show that NLRX1 negatively regulates IEC proliferation during the epithelial regeneration phase following intestinal injury.

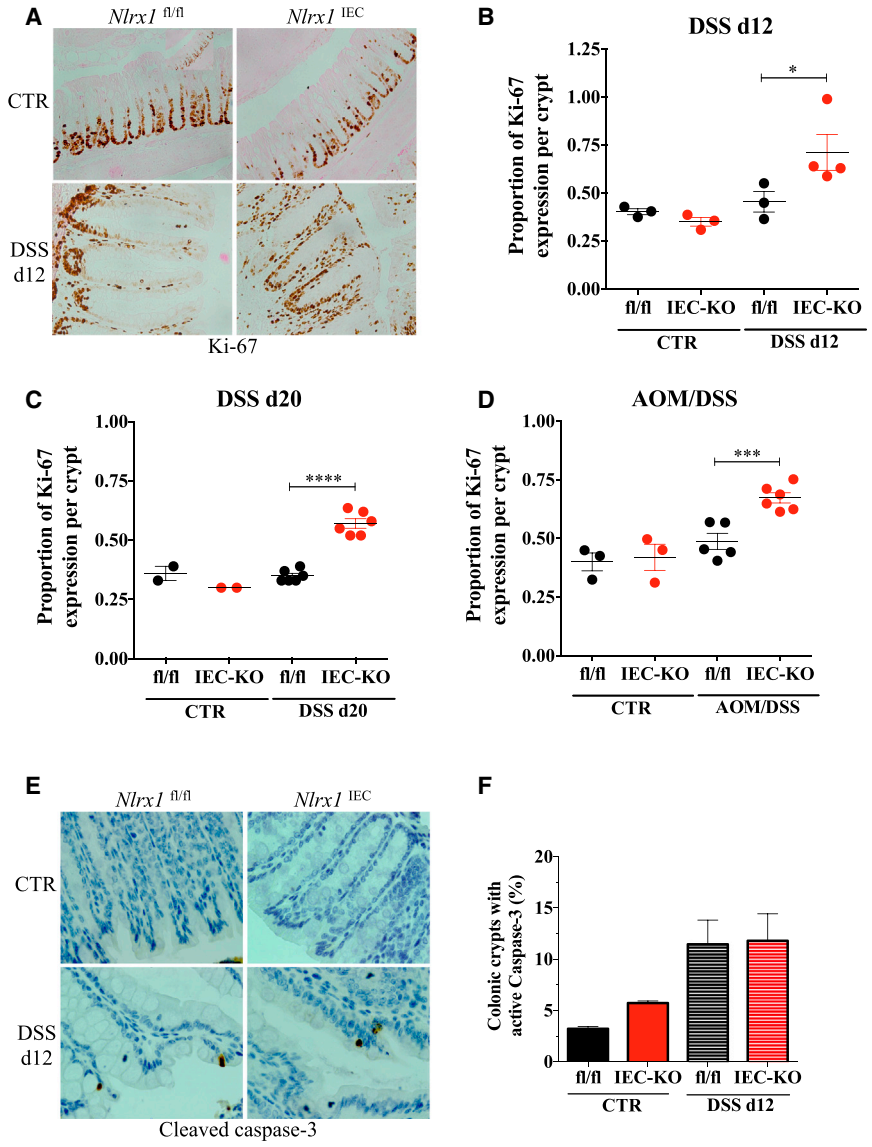

Figure 5. Increased Epithelial Proliferation in *Nlrx1*$^{\Delta IEC}$ Mice during Epithelial Regeneration

(A) IHC using anti-Ki-67 antibody of colonic sections of *Nlrx1*$^{fl/fl}$ and *Nlrx1* $^{\Delta IEC}$ mice unchallenged (CTR) or challenged with 2.5% DSS at d12 (5 days DSS/7 days recovery).

(B–D) Quantification of the average proportion of the crypt length that is Ki-67^{+} at post-DSS d12 (B), d20 (C), or animals challenged with AOM/DSS (D). Each point represents the quantification of n ≥ 100 crypts of one animal.

(E and F) Representative IHC micrographs (E) and quantification (F) or colonic sections at d12 post-DSS using an antibody against the cleaved caspase-3.

TNF stimulation was caused, at least in part, by hyperproliferation.

Intestinal organoids grow from rapidly dividing pluripotent intestinal stem cells (ISCs) that are found at the bottom of the crypts and express the marker *Lgr5* (Barker et al., 2007). Another ISC population, likely acting as a reserve ISC, expresses *Bmi1* (Sangiorgi and Capecchi, 2008; Tian et al., 2011). Cells leaving the ISC niche lose expression of the *Lgr5* and *Bmi1* markers and form the transit-amplifying (TA) zone, in which cells remain highly proliferative and still express numerous ISC markers, but progressively differentiate into specific IEC populations. qPCR analysis revealed that stimulation with TNF resulted in a modest increase in the expression of *Lgr5* and *Bmi1* in intestinal organoids from both *Nlrx1*$^{\Delta IEC}$ and *Nlrx1*$^{fl/fl}$ mice; however, this increase was not significantly different between the two groups of organoids (Figures S4A and S4B). Next, we analyzed the expression of *Olfm4*, an ISC marker that, in contrast to *Bmi1* and *Lgr5*, remains expressed in the TA zone (Itzkovitz et al., 2012). Interestingly, we observed stronger upregulation of *Olfm4* in organoids from *Nlrx1*$^{\Delta IEC}$ than those from *Nlrx1*$^{fl/fl}$ mice following TNF stimulation (Figure 6E), suggesting that NLRX1 specifically represses proliferation of cells in the TA zone, rather than cells in the ISC niche.

Uncontrolled proliferation of cells in the ISC niche or the TA zone can drive tumorigenesis. It was shown that the transcription factor *Myb*, which is highly expressed in ISCs (Muñoz et al., 2012), was required for proliferation in colonic crypts (Malaterre et al., 2007) and *Myb* activation results in colon tumorigenesis in mice (Malaterre et al., 2015). Strikingly, TNF stimulation resulted in only a transient upregulation of *Myb* expression in organoids from *Nlrx1*$^{fl/fl}$ mice, while this upregulation persisted in those from *Nlrx1*$^{\Delta IEC}$ mice (Figure 6F). Thus, dysregulated expression of *Myb* in the colonic crypts of *Nlrx1*$^{\Delta IEC}$ mice during epithelial restitution following injury could contribute to the exacerbated tumorigenesis observed in these mice in the AOM/DSS model.

We have demonstrated above that epithelial regeneration following DSS-induced injury resulted in exacerbated expression of *Tnf*, *Egf*, and *Tgfb1* in *Nlrx1*$^{\Delta IEC}$ mice as compared to *Nlrx1*$^{fl/fl}$ mice, suggesting that these factors could be expressed by the intestinal epithelium itself, since non-IECs in both groups of mice are WT. In support for this, we observed that stimulation of organoids from *Nlrx1*$^{\Delta IEC}$ and *Nlrx1*$^{fl/fl}$ mice with TNF resulted in potent transcriptional upregulation of both *Tnf* and *Tgfb1* (Figures 6G and 6H), as well as a more modest induction of *Egf* (Figure S4C). In contrast, *Il6* transcript was undetectable in these conditions (data not shown). Therefore, these data support the notion that *Tnf*, *Tgfb1*, and *Egf* can be expressed through paracrine regulation by the intestinal epithelium.

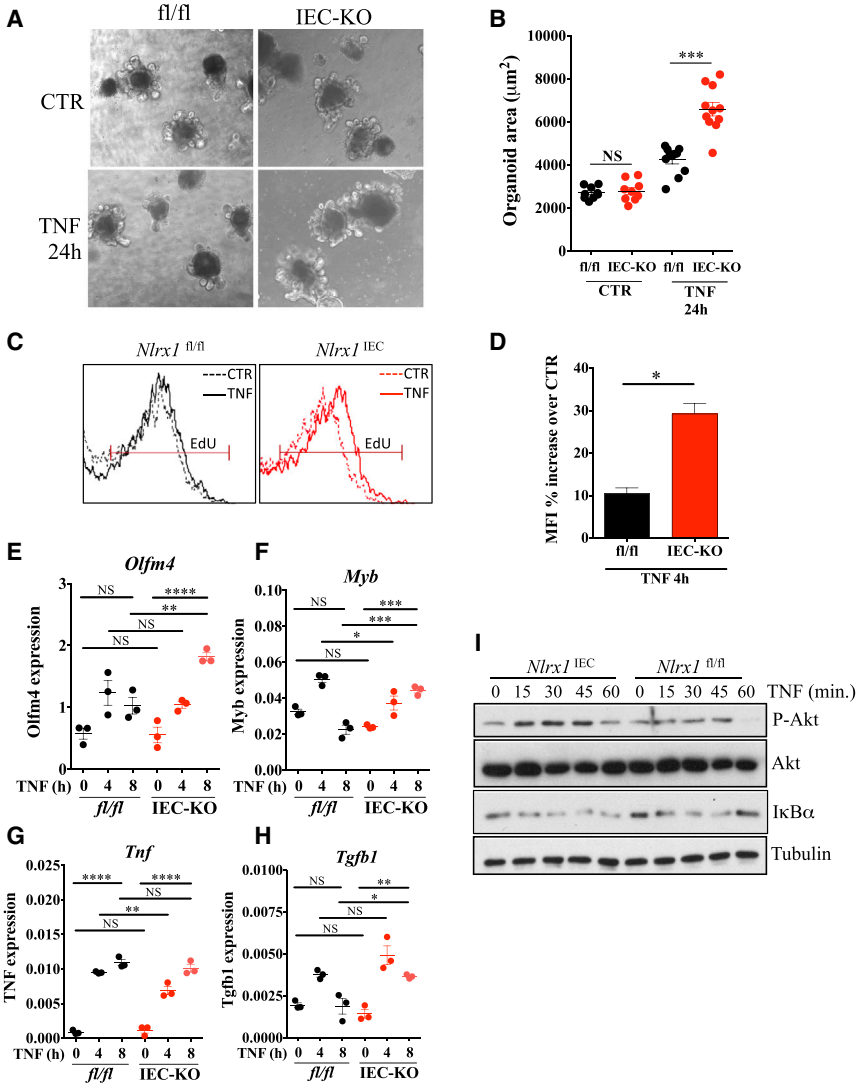

Figure 6. Expression of NLRX1 Inhibits TNF-Mediated Proliferation and Signalization in Primary Intestinal Organoids

(A and B) Representative bright field micrographs (A) and quantification of the surface (B) of intestinal organoids derived from *Nlrx1*$^{fl/fl}$ (fl/fl) and *Nlrx1* $^{\Delta IEC}$ (IEC-KO) mice in normal growth media supplemented or not with TNF at 10 ng/ml for 24 hr. For quantifications, each point represents the average surface area of all the organoids found in one individual culture well. The results are representative of two independent experiments.

(C and D) Analysis by flow cytometry (C) and quantification of the average mean fluorescence intensity (MFI) (D) of EdU incorporation in fl/fl and IEC-KO organoids stimulated or not with TNF at 10 ng/ml for 4 hr. The results are representative of three independent experiments.

(E–H) qPCR analysis of the expression of *Olfm4* (E), *Myb* (F), *Tnf* (G), or *Tgfb1* (H) in fl/fl and IEC-KO organoids stimulated or not with TNF at 10 ng/ml for 4 or 8 hr. Each point represents the average value for technical triplicate of individual organoid cultures derived from different mice.

(I) Western blot analysis of fl/fl and IEC-KO organoids stimulated or not with TNF at 10 ng/ml for 15 to 60 min. The blots are representative of two independent experiments (*$p < 0.05$; **$p < 0.01$; ***$p < 0.001$; and ****$p < 0.0001$) (non-significant, NS).

In order to better understand the mechanism through which TNF triggered a hyper-proliferative response in organoids from *Nlrx1*$^{\Delta IEC}$ mice, we analyzed by western blotting the activation of Akt, a protein that plays a central role in the regulation of epithelial cell proliferation (Lee et al., 2010) and whose dysregulation is strongly associated with colorectal cancer (Agarwal et al., 2013; Leystra et al., 2012). TNF stimulation resulted in rapid upregulation of Akt phosphorylation in both groups of organoids; however, the effect was stronger and more sustained in organoids from *Nlrx1*$^{\Delta IEC}$ mice than those from *Nlrx1*$^{fl/fl}$ mice (Figure 6I). Finally, we analyzed NF-κB signaling, since this pathway is also critical for the control of IEC proliferation and intestinal tumorigenesis (Myant et al., 2013; Steinbrecher et al., 2008). Similar to Akt activation, we observed that TNF stimulation triggered degradation of the inhibitory molecule Iκbα, which indicates NF-κB activation, in both groups of organoids, but the effect was again more sustained in organoids from *Nlrx1*$^{\Delta IEC}$ mice than those from *Nlrx1*$^{fl/fl}$ mice (Figure 6I). Together, these results indicate that TNF-mediated hyper-proliferative response in organoids from *Nlrx1*$^{\Delta IEC}$ mice was associated with exacerbated activation of the Akt and NF-κB signaling pathways and upregulation of the transcription factor Myb.

DISCUSSION

Chronic injury of the intestinal mucosa can favor the development of colorectal cancer. This is highlighted by the fact that inflammatory bowel disease confers increased risk of developing gastrointestinal neoplasia in humans. Similarly, repeated exposure to the epithelial irritant DSS greatly accelerates tumor formation in the AOM/DSS model in mice (Rosenberg et al., 2009). It is clear that inflammation plays a critical role in this effect, and inflammation-associated cytokines such as IL-6 are known to contribute to the pathogenesis of colorectal cancer (Waldner and Neurath, 2014). However, it is less appreciated that epithelial regeneration and wound repair pathways, which are triggered as a direct consequence of mucosal injury and are amplified by inflammatory mediators, likely play central roles in colitis-associated intestinal tumorigenesis. Indeed, these important processes rely on cellular proliferation and migration and on signaling pathways dependent on NF-κB, Akt/PI3K, and Wnt/β-catenin, all of which being critical actors of colorectal cancer pathogenesis. Because inflammation and epithelial repair pathways are tightly interconnected and are spatially and temporally coordinated, it is difficult to determine what aspects of inflammation (i.e., recruitment of immune cells, upregulation of phagocytosis, secretion of inflammatory or

immune defense mediators, microbiota dysbiosis, and upregulation of epithelial repair) have the most important impact on tumorigenesis. One way to approach this question and to identify key molecular pathways linking specific arms of inflammation to tumorigenesis is to perform analysis of mice with tissue-specific gene deletion. Here, by using mice harboring a deletion of *Nlrx1* only in IECs, we identified an epithelial-intrinsic role for this NLR molecule in the control of IEC proliferation during the epithelial regeneration phase following DSS treatment. Our data suggest that *Nlrx1* deletion exacerbates cellular responses to TNF, which could generate a paracrine or autocrine amplification loop in IECs by triggering *Tnf* expression. This effect might also amplify the expression of other wound healing genes, such as *Tgfb1* and *Egf*, as suggested by our results in intestinal organoids. Thus, our data suggest that, by restricting the activation of Akt and NF-κB in IECs in response to TNF stimulation, NLRX1 tones down the effect of TNF on the proliferation of TA cells in the intestinal crypt, providing a protection against colitis-associated tumorigenesis. It is possible that a similar mechanism underlies the protective role of NLRX1 against tumorigenesis in mice carrying the Apc^{min} mutation, since increased mucosal expression of *Tnf* was observed in these mice and correlated with tumor formation (McClellan et al., 2012).

Our previous results demonstrated that full-body deletion of *Nlrx1* resulted in increased inflammation following DSS treatment (Soares et al., 2014), which is in line with other studies showing an inhibitory effect of NLRX1 on inflammation (Allen et al., 2011; Xia et al., 2011; Eitas et al., 2014; Kang et al., 2015). Although this effect is likely immune cell-intrinsic, the underlying mechanism is not clearly elucidated, nor are the immune cell subsets identified that are undergoing uncontrolled activation in *Nlrx1*-deficient mice. Nevertheless, these observations, together with the results of the present study, suggest that NLRX1 might mitigate colitis-associated tumorigenesis at two levels: (1) by downregulating inflammation and (2) by inhibiting pro-proliferative responses in the intestinal epithelium in response to inflammatory and pro-regeneration cues.

Our data show that, in intestinal organoids, NLRX1 diminishes TNF-induced activation of both Akt- and NF-κB-dependent pathways. Since Akt was shown to be essential for TNF-mediated activation of NF-κB (Ozes et al., 1999), it is likely that the primary effect of NLRX1 is at the level of Akt signaling. Alternatively, NLRX1 could regulate a step or an event that controls both pathways, such as mitochondrial ROS levels or expression of TNF receptors. Future studies will aim at identifying the molecular mechanism by which NLRX1 mitigates Akt and NF-κB signaling in response to TNF stimulation in IECs.

Overall, our study identifies an epithelial-intrinsic role for NLRX1 in the control of colon tumorigenesis through the modulation of epithelial proliferation following injury. Experiments in primary intestinal organoids further revealed that NLRX1 directly impacted Akt and NF-κB pathways, expression of the proliferation-associated transcription factor Myb, and proliferation of crypt TA cells in response to TNF. Identifying the mechanism through which NLRX1 controls these pathways will allow the designing of novel therapeutic strategies aimed at regulating hyper-proliferative responses in colon cancer without having to suppress inflammatory cytokine networks.

EXPERIMENTAL PROCEDURES

Animals

All mice were bred and housed at the Division of Clinical Medicine (DCM) of the University of Toronto and experiments were performed according to guidelines of the DCM and following protocols approved by the University of Toronto Committee on Use and Care of Animals. Mice were kept in specific pathogen-free conditions with periodic testing for murine norovirus and used for experiments at age 6–10 weeks except otherwise indicated. All experiments were performed using littermate animals that were separated at weaning. $Nlrx1^{-/-}$ mice have been described previously (Soares et al., 2013).

Generation of IEC-Specific NLRX1-Deficient Mice

NLRX1-deficient mice ($Nlrx1^{\Delta IEC}$) were generated by crossing $Nlrx1^{fl/fl}$ mice (Soares et al., 2013) with transgenic mice *B6.SJL-Tg(Vil-cre)997Gum/J* (Jackson Laboratories), which express Cre recombinase under the control of the mouse *villin* promoter. The following PCR primers (5′–3′) were used to genotype WT, floxed, and $Nlrx1^{\Delta IEC}$ mice: primer 1- (CCA TTT GCC AAT CCC ACT CAC), primer 2 (ACC AAG AAC CTA ACC CAC GGT C), primer 3 (TTG CCA GCC ATC TGT TGT TTG), oIMR1878 (GTG TGG GAC AGA GAA CAA ACC), and oIMR1879 (ACA TCT TCA GGT TCT GCG GG).

Induction of DSS-Induced Colitis

Colitis was induced with 2.5% (w/v) DSS (MP Biomedicals) dissolved in sterile, distilled water for experimental days 5, followed by normal drinking water until the end of the experiment.

Colitis-Associated Colorectal Cancer

Mice were injected intraperitoneally with 10 mg/kg AOM (Sigma-Aldrich). After 5 days, 2.5% DSS was given in drinking water over 5 days, followed by regular drinking water for 2 weeks. This cycle was repeated three times, and mice were sacrificed 2 weeks after the last DSS cycle. The experiments were performed with at least 4–8 mice in each AOM-treated condition.

Reagents and Antibodies

AOM (Sigma-Aldrich, A5486). DSS (MP Biomedicals, 160110). The following antibodies were used for protein detection: rabbit polyclonal AKT rabbit polyclonal (Cell Signaling Technology, 9272S), rabbit polyclonal Phospho-AKT (Ser473) (Cell Signaling Technology, 9271S), rabbit polyclonal anti-cleaved caspase-3 (Asp175) (Cell Signaling Technology, 9661S), rabbit anti-chromogranin A (Abcam, ab15160), rabbit anti-Muc2 (H300) (Santa Cruz, sc-15334) mouse monoclonal anti-tubulin (Sigma-Aldrich, T9026), rabbit polyclonal anti-Ki-67 (D3B5) (Cell Signaling Technology, 12202), mouse monoclonal anti-NLRX1 (Millipore, 04-146) and rabbit monoclonal anti-IκB-α (E130) (Abcam, ab32518), goat anti-rabbit (ThermoScientific / Molecular Probes, A-21245), AB solution (Sigma-Aldrich, B8438), Periodic Acid- Schiff (PAS) kit (Sigma-Aldrich, 395B), Alexa Fluor 647 donkey anti-rabbit (Life Technologies, A31573), and Click-iT EdU Flow Cytometry Assay Kit (Life Technologies, C10419).

Statistical Analysis

Prism software was used to plot data and determine statistical significance using a Student's t test (for two groups) or ANOVA for data sets with three or more sets of data to analyze. Data are presented as means ± SEM. A p value of <0.05 was considered to be statistically significant.

SUPPLEMENTAL INFORMATION

Supplemental Information includes Supplemental Experimental Procedures, four figures, and one table and can be found with this article online at http://dx.doi.org/10.1016/j.celrep.2016.02.065.

AUTHOR CONTRIBUTIONS

I.T., D.J.P., and S.E.G. designed the study and analyzed data. I.T. performed most experiments of the study. S.E.G. wrote the manuscript. S.A.K. and

M.A.R. performed western blots, E.G.F. performed immunofluorescence, R.M. did EdU assays, and C.M. performed some qPCRs. S.W., D.A.W., and C.J.S. performed blinded pathological scoring.

ACKNOWLEDGMENTS

This project is supported in part by the Nick Natale Innovation Grant of the Canadian Cancer Society (grant #702392) (to S.E.G.), the Natural Sciences and Engineering Research Council of Canada (to S.E.G.), and from a team grant from the Canadian Institutes of Health Research on NLRs and inflammation (to D.J.P. and S.E.G.). We thank Dr. Sheila Costford for some of the statistical analyses and Dr. A. Martin (University of Toronto) for providing the $Apc^{min/+}$ mice.

Received: January 4, 2016
Revised: February 8, 2016
Accepted: February 22, 2016
Published: March 10, 2016

REFERENCES

Agarwal, E., Brattain, M.G., and Chowdhury, S. (2013). Cell survival and metastasis regulation by Akt signaling in colorectal cancer. Cell. Signal. *25*, 1711–1719.

Allen, I.C., Moore, C.B., Schneider, M., Lei, Y., Davis, B.K., Scull, M.A., Gris, D., Roney, K.E., Zimmermann, A.G., Bowzard, J.B., et al. (2011). NLRX1 protein attenuates inflammatory responses to infection by interfering with the RIG-I-MAVS and TRAF6-NF-κB signaling pathways. Immunity *34*, 854–865.

Arnoult, D., Soares, F., Tattoli, I., Castanier, C., Philpott, D.J., and Girardin, S.E. (2009). An N-terminal addressing sequence targets NLRX1 to the mitochondrial matrix. J. Cell Sci. *122*, 3161–3168.

Barker, N., van Es, J.H., Kuipers, J., Kujala, P., van den Born, M., Cozijnsen, M., Haegebarth, A., Korving, J., Begthel, H., Peters, P.J., and Clevers, H. (2007). Identification of stem cells in small intestine and colon by marker gene Lgr5. Nature *449*, 1003–1007.

Danielsson, F., Skogs, M., Huss, M., Rexhepaj, E., O'Hurley, G., Klevebring, D., Pontén, F., Gad, A.K., Uhlén, M., and Lundberg, E. (2013). Majority of differentially expressed genes are down-regulated during malignant transformation in a four-stage model. Proc. Natl. Acad. Sci. USA *110*, 6853–6858.

Eitas, T.K., Chou, W.C., Wen, H., Gris, D., Robbins, G.R., Brickey, J., Oyama, Y., and Ting, J.P. (2014). The nucleotide-binding leucine-rich repeat (NLR) family member NLRX1 mediates protection against experimental autoimmune encephalomyelitis and represses macrophage/microglia-induced inflammation. J. Biol. Chem. *289*, 4173–4179.

Hu, X., Chung, A.Y., Wu, I., Foldi, J., Chen, J., Ji, J.D., Tateya, T., Kang, Y.J., Han, J., Gessler, M., et al. (2008). Integrated regulation of Toll-like receptor responses by Notch and interferon-gamma pathways. Immunity *29*, 691–703.

Imbeault, E., Mahvelati, T.M., Braun, R., Gris, P., and Gris, D. (2014). Nlrx1 regulates neuronal cell death. Mol. Brain *7*, 90.

Itzkovitz, S., Lyubimova, A., Blat, I.C., Maynard, M., van Es, J., Lees, J., Jacks, T., Clevers, H., and van Oudenaarden, A. (2012). Single-molecule transcript counting of stem-cell markers in the mouse intestine. Nat. Cell Biol. *14*, 106–114.

Jaworska, J., Coulombe, F., Downey, J., Tzelepis, F., Shalaby, K., Tattoli, I., Berube, J., Rousseau, S., Martin, J.G., Girardin, S.E., et al. (2014). NLRX1 prevents mitochondrial induced apoptosis and enhances macrophage antiviral immunity by interacting with influenza virus PB1-F2 protein. Proc. Natl. Acad. Sci. USA *111*, E2110–E2119.

Kang, M.J., Yoon, C.M., Kim, B.H., Lee, C.M., Zhou, Y., Sauler, M., Homer, R., Dhamija, A., Boffa, D., West, A.P., et al. (2015). Suppression of NLRX1 in chronic obstructive pulmonary disease. J. Clin. Invest. *125*, 2458–2462.

Lee, G., Goretsky, T., Managlia, E., Dirisina, R., Singh, A.P., Brown, J.B., May, R., Yang, G.Y., Ragheb, J.W., Evers, B.M., et al. (2010). Phosphoinositide 3-kinase signaling mediates beta-catenin activation in intestinal epithelial stem and progenitor cells in colitis. Gastroenterology *139*, 869–881.

Leppkes, M., Roulis, M., Neurath, M.F., Kollias, G., and Becker, C. (2014). Pleiotropic functions of TNF-α in the regulation of the intestinal epithelial response to inflammation. Int. Immunol. *26*, 509–515.

Leystra, A.A., Deming, D.A., Zahm, C.D., Farhoud, M., Olson, T.J., Hadac, J.N., Nettekoven, L.A., Albrecht, D.M., Clipson, L., Sullivan, R., et al. (2012). Mice expressing activated PI3K rapidly develop advanced colon cancer. Cancer Res. *72*, 2931–2936.

Malaterre, J., Carpinelli, M., Ernst, M., Alexander, W., Cooke, M., Sutton, S., Dworkin, S., Heath, J.K., Frampton, J., McArthur, G., et al. (2007). c-Myb is required for progenitor cell homeostasis in colonic crypts. Proc. Natl. Acad. Sci. USA *104*, 3829–3834.

Malaterre, J., Pereira, L., Putoczki, T., Millen, R., Paquet-Fifield, S., Germann, M., Liu, J., Cheasley, D., Sampurno, S., Stacker, S.A., et al. (2015). Intestinal-specific activatable Myb initiates colon tumorigenesis in mice. Oncogene. http://dx.doi.org/10.1038/onc.2015.305.

McClellan, J.L., Davis, J.M., Steiner, J.L., Day, S.D., Steck, S.E., Carmichael, M.D., and Murphy, E.A. (2012). Intestinal inflammatory cytokine response in relation to tumorigenesis in the Apc(Min/+) mouse. Cytokine *57*, 113–119.

Moore, C.B., Bergstralh, D.T., Duncan, J.A., Lei, Y., Morrison, T.E., Zimmermann, A.G., Accavitti-Loper, M.A., Madden, V.J., Sun, L., Ye, Z., et al. (2008). NLRX1 is a regulator of mitochondrial antiviral immunity. Nature *451*, 573–577.

Muñoz, J., Stange, D.E., Schepers, A.G., van de Wetering, M., Koo, B.K., Itzkovitz, S., Volckmann, R., Kung, K.S., Koster, J., Radulescu, S., et al. (2012). The Lgr5 intestinal stem cell signature: robust expression of proposed quiescent '+4' cell markers. EMBO J. *31*, 3079–3091.

Myant, K.B., Cammareri, P., McGhee, E.J., Ridgway, R.A., Huels, D.J., Cordero, J.B., Schwitalla, S., Kalna, G., Ogg, E.L., Athineos, D., et al. (2013). ROS production and NF-κB activation triggered by RAC1 facilitate WNT-driven intestinal stem cell proliferation and colorectal cancer initiation. Cell Stem Cell *12*, 761–773.

Ozes, O.N., Mayo, L.D., Gustin, J.A., Pfeffer, S.R., Pfeffer, L.M., and Donner, D.B. (1999). NF-kappaB activation by tumour necrosis factor requires the Akt serine-threonine kinase. Nature *401*, 82–85.

Philpott, D.J., Sorbara, M.T., Robertson, S.J., Croitoru, K., and Girardin, S.E. (2014). NOD proteins: regulators of inflammation in health and disease. Nat. Rev. Immunol. *14*, 9–23.

Raskov, H., Pommergaard, H.C., Burcharth, J., and Rosenberg, J. (2014). Colorectal carcinogenesis–update and perspectives. World J. Gastroenterol. *20*, 18151–18164.

Rebsamen, M., Vazquez, J., Tardivel, A., Guarda, G., Curran, J., and Tschopp, J. (2011). NLRX1/NOD5 deficiency does not affect MAVS signalling. Cell Death Differ. *18*, 1387.

Rosenberg, D.W., Giardina, C., and Tanaka, T. (2009). Mouse models for the study of colon carcinogenesis. Carcinogenesis *30*, 183–196.

Sangiorgi, E., and Capecchi, M.R. (2008). Bmi1 is expressed in vivo in intestinal stem cells. Nat. Genet. *40*, 915–920.

Sato, T., Vries, R.G., Snippert, H.J., van de Wetering, M., Barker, N., Stange, D.E., van Es, J.H., Abo, A., Kujala, P., Peters, P.J., and Clevers, H. (2009). Single Lgr5 stem cells build crypt-villus structures in vitro without a mesenchymal niche. Nature *459*, 262–265.

Singh, K., Poteryakhina, A., Zheltukhin, A., Bhatelia, K., Prajapati, P., Sripada, L., Tomar, D., Singh, R., Singh, A.K., Chumakov, P.M., and Singh, R. (2015). NLRX1 acts as tumor suppressor by regulating TNF-α induced apoptosis and metabolism in cancer cells. Biochim. Biophys. Acta *1853*, 1073–1086.

Soares, F., Tattoli, I., Wortzman, M.E., Arnoult, D., Philpott, D.J., and Girardin, S.E. (2013). NLRX1 does not inhibit MAVS-dependent antiviral signalling. Innate Immun. *19*, 438–448.

Soares, F., Tattoli, I., Rahman, M.A., Robertson, S.J., Belcheva, A., Liu, D., Streutker, C., Winer, S., Winer, D.A., Martin, A., et al. (2014). The mitochondrial

protein NLRX1 controls the balance between extrinsic and intrinsic apoptosis. J. Biol. Chem. *289*, 19317–19330.

Steinbrecher, K.A., Harmel-Laws, E., Sitcheran, R., and Baldwin, A.S. (2008). Loss of epithelial RelA results in deregulated intestinal proliferative/apoptotic homeostasis and susceptibility to inflammation. J. Immunol. *180*, 2588–2599.

Sturm, A., and Dignass, A.U. (2008). Epithelial restitution and wound healing in inflammatory bowel disease. World J. Gastroenterol. *14*, 348–353.

Su, L.K., Kinzler, K.W., Vogelstein, B., Preisinger, A.C., Moser, A.R., Luongo, C., Gould, K.A., and Dove, W.F. (1992). Multiple intestinal neoplasia caused by a mutation in the murine homolog of the APC gene. Science *256*, 668–670.

Tattoli, I., Carneiro, L.A., Jéhanno, M., Magalhaes, J.G., Shu, Y., Philpott, D.J., Arnoult, D., and Girardin, S.E. (2008). NLRX1 is a mitochondrial NOD-like receptor that amplifies NF-kappaB and JNK pathways by inducing reactive oxygen species production. EMBO Rep. *9*, 293–300.

Tian, H., Biehs, B., Warming, S., Leong, K.G., Rangell, L., Klein, O.D., and de Sauvage, F.J. (2011). A reserve stem cell population in small intestine renders Lgr5-positive cells dispensable. Nature *478*, 255–259.

Waldner, M.J., and Neurath, M.F. (2014). Master regulator of intestinal disease: IL-6 in chronic inflammation and cancer development. Semin. Immunol. *26*, 75–79.

Xia, X., Cui, J., Wang, H.Y., Zhu, L., Matsueda, S., Wang, Q., Yang, X., Hong, J., Songyang, Z., Chen, Z.J., and Wang, R.F. (2011). NLRX1 negatively regulates TLR-induced NF-κB signaling by targeting TRAF6 and IKK. Immunity *34*, 843–853.